ISSN 1007-9327 (print)
ISSN 2219-2840 (online)

World Journal of *Gastroenterology*

World J Gastroenterol 2024 March 14; 30(10): 1261-1469

Published by Baishideng Publishing Group Inc

World Journal of Gastroenterology

Contents

Weekly Volume 30 Number 10 March 14, 2024

EDITORIAL

REVIEW

ORIGINAL ARTICLE

Retrospective Cohort Study

World Journal of Gastroenterology

Weekly Volume 30 Number 10 March 14, 2024

Contents

Contents

ABOUT COVER

Editorial Board Member of *World Journal of Gastroenterology*, Toru Mizuguchi, MD, PhD, Professor, Surgeon, Department of Nursing, Division of Surgical Science, Sapporo Medical University Postgraduate School of Health Science, Sapporo, Hokkaido 0608556, Japan. tmizu@sapmed.ac.jp

AIMS AND SCOPE

The primary aim of *World Journal of Gastroenterology* (*WJG*, *World J Gastroenterol*) is to provide scholars and readers from various fields of gastroenterology and hepatology with a platform to publish high-quality basic and clinical research articles and communicate their research findings online. *WJG* mainly publishes articles reporting research results and findings obtained in the field of gastroenterology and hepatology and covering a wide range of topics including gastroenterology, hepatology, gastrointestinal endoscopy, gastrointestinal surgery, gastrointestinal oncology, and pediatric gastroenterology.

INDEXING/ABSTRACTING

The *WJG* is now abstracted and indexed in Science Citation Index Expanded (SCIE), MEDLINE, PubMed, PubMed Central, Scopus, Reference Citation Analysis, China Science and Technology Journal Database, and Superstar Journals Database. The 2023 edition of Journal Citation Reports® cites the 2022 impact factor (IF) for *WJG* as 4.3; Quartile category: Q2. The *WJG*'s CiteScore for 2021 is 8.3.

RESPONSIBLE EDITORS FOR THIS ISSUE

NAME OF JOURNAL
World Journal of Gastroenterology

ISSN
ISSN 1007-9327 (print) ISSN 2219-2840 (online)

LAUNCH DATE
October 1, 1995

FREQUENCY
Weekly

PUBLICATION DATE
March 14, 2024

PUBLISHING PARTNER
Shanghai Pancreatic Cancer Institute and Pancreatic Cancer Institute, Fudan University
Biliary Tract Disease Institute, Fudan University

INSTRUCTIONS TO AUTHORS
https://www.wjgnet.com/bpg/gerinfo/204

GUIDELINES FOR ETHICS DOCUMENTS
https://www.wjgnet.com/bpg/GerInfo/287

GUIDELINES FOR NON-NATIVE SPEAKERS OF ENGLISH
https://www.wjgnet.com/bpg/gerinfo/240

PUBLICATION ETHICS
https://www.wjgnet.com/bpg/GerInfo/288

PUBLICATION MISCONDUCT
https://www.wjgnet.com/bpg/gerinfo/208

POLICY OF CO-AUTHORS
https://www.wjgnet.com/bpg/GerInfo/310

ARTICLE PROCESSING CHARGE
https://www.wjgnet.com/bpg/gerinfo/242

STEPS FOR SUBMITTING MANUSCRIPTS
https://www.wjgnet.com/bpg/GerInfo/239

ONLINE SUBMISSION
https://www.f6publishing.com

PUBLISHING PARTNER's OFFICIAL WEBSITE
https://www.shca.org.cn
https://www.zs-hospital.sh.cn

World Journal of Gastroenterology

Submit a Manuscript: https://www.f6publishing.com

World J Gastroenterol 2024 March 14; 30(10): 1405-1419

DOI: 10.3748/wjg.v30.i10.1405

ISSN 1007-9327 (print) ISSN 2219-2840 (online)

ORIGINAL ARTICLE

Basic Study

Alkaline sphingomyelinase deficiency impairs intestinal mucosal barrier integrity and reduces antioxidant capacity in dextran sulfate sodium-induced colitis

Ye Tian, Xin Li, Xu Wang, Si-Ting Pei, Hong-Xin Pan, Yu-Qi Cheng, Yi-Chen Li, Wen-Ting Cao, Jin-Dong Ding Petersen, Ping Zhang

Specialty type: Gastroenterology and hepatology

Provenance and peer review: Unsolicited article; Externally peer reviewed.

Peer-review model: Single blind

Peer-review report's scientific quality classification

Grade A (Excellent): 0
Grade B (Very good): B
Grade C (Good): C
Grade D (Fair): 0
Grade E (Poor): 0

P-Reviewer: Diener M, Germany

Received: October 12, 2023
Peer-review started: October 12, 2023
First decision: December 8, 2023
Revised: December 26, 2023
Accepted: January 29, 2024
Article in press: January 29, 2024
Published online: March 14, 2024

Ye Tian, Si-Ting Pei, Hong-Xin Pan, Wen-Ting Cao, Jin-Dong Ding Petersen, Ping Zhang, International School of Public Health and One Health, Hainan Medical University, Haikou 571199, Hainan Province, China

Xin Li, Yu-Qi Cheng, Yi-Chen Li, Medical Laboratory Science and Technology College, Harbin Medical University - Daqing Campus, Daqing 163000, Heilongjiang Province, China

Xu Wang, Department of Laboratory Diagnosis, Qiqihar Tuberculosis Control Center, Qiqihar 161000, Heilongjiang Province, China

Jin-Dong Ding Petersen, Department of Public Health, University of Copenhagen, Copenhagen 1353, Denmark

Jin-Dong Ding Petersen, Department of Public Health, University of Southern Denmark, Odense 5000, Denmark

Corresponding author: Ping Zhang, MD, PhD, Professor, International School of Public Health and One Health, Hainan Medical University, No. 3 Xueyuan Road, Haikou 571199, Hainan Province, China. pingzhang@hainmc.edu.cn

Abstract

BACKGROUND

Ulcerative colitis is a chronic inflammatory disease of the colon with an unknown etiology. Alkaline sphingomyelinase (alk-SMase) is specifically expressed by intestinal epithelial cells, and has been reported to play an anti-inflammatory role. However, the underlying mechanism is still unclear.

AIM

To explore the mechanism of alk-SMase anti-inflammatory effects on intestinal barrier function and oxidative stress in dextran sulfate sodium (DSS)-induced colitis.

METHODS

Mice were administered 3% DSS drinking water, and disease activity index was determined to evaluate the status of colitis. Intestinal permeability was evaluated

by gavage administration of fluorescein isothiocyanate dextran, and bacterial translocation was evaluated by measuring serum lipopolysaccharide. Intestinal epithelial cell ultrastructure was observed by electron microscopy. Western blotting and quantitative real-time reverse transcription-polymerase chain reaction were used to detect the expression of intestinal barrier proteins and mRNA, respectively. Serum oxidant and antioxidant marker levels were analyzed using commercial kits to assess oxidative stress levels.

RESULTS

Compared to wild-type (WT) mice, inflammation and intestinal permeability in alk-SMase knockout (KO) mice were more severe beginning 4 d after DSS induction. The mRNA and protein levels of intestinal barrier proteins, including zonula occludens-1, occludin, claudin-3, claudin-5, claudin-8, mucin 2, and secretory immunoglobulin A, were significantly reduced on 4 d after DSS treatment. Ultrastructural observations revealed progressive damage to the tight junctions of intestinal epithelial cells. Furthermore, by day 4, mitochondria appeared swollen and degenerated. Additionally, compared to WT mice, serum malondialdehyde levels in KO mice were higher, and the antioxidant capacity was significantly lower. The expression of the transcription factor nuclear factor erythroid 2-related factor 2 (Nrf2) in the colonic mucosal tissue of KO mice was significantly decreased after DSS treatment. mRNA levels of Nrf2-regulated downstream antioxidant enzymes were also decreased. Finally, colitis in KO mice could be effectively relieved by the injection of tertiary butylhydroquinone, which is an Nrf2 activator.

CONCLUSION

Alk-SMase regulates the stability of the intestinal mucosal barrier and enhances antioxidant activity through the Nrf2 signaling pathway.

Key Words: Alkaline sphingomyelinase; Intestinal mucosal barrier; Antioxidant capacity; Dextran sulfate sodium-induced colitis; nuclear factor erythroid 2-related factor 2

Core Tip: The protective effect of alkaline sphingomyelinase (alk-SMase) against intestinal inflammation has been demonstrated, but the underlying molecular mechanism remains unclear. In the present study, we found that alk-SMase deficiency exacerbated damage to the intestinal mucosal barrier in dextran sulfate sodium-induced colitis. Additionally, alk-SMase was shown to enhance antioxidant activity, thereby reducing susceptibility to proinflammatory factors in colitis. Furthermore, our findings revealed that alk-SMase may maintain intestinal barrier stability and increase antioxidant capacity through the nuclear factor erythroid 2-related factor 2 signaling pathway.

Citation: Tian Y, Li X, Wang X, Pei ST, Pan HX, Cheng YQ, Li YC, Cao WT, Petersen JDD, Zhang P. Alkaline sphingomyelinase deficiency impairs intestinal mucosal barrier integrity and reduces antioxidant capacity in dextran sulfate sodium-induced colitis. *World J Gastroenterol* 2024; 30(10): 1405-1419
URL: https://www.wjgnet.com/1007-9327/full/v30/i10/1405.htm
DOI: https://dx.doi.org/10.3748/wjg.v30.i10.1405

INTRODUCTION

Ulcerative colitis (UC), which is a kind of inflammatory bowel disease (IBD), is a chronic and recurrent inflammatory disease of the colon that causes destruction and inflammation in the colonic mucosa and a persistent increase in the risk of developing colorectal cancer (CRC)[1,2]. However, the etiology of UC is unclear, and it is believed that UC is related to many factors, such as genetics, the environment, infection and immunomodulatory disorders, and damage to the intestinal mucosal barrier is the core of its pathogenesis[3]. The intestinal mucosal barrier includes the mechanical barrier, immune barrier, microbial barrier and chemical barrier. Any instability in intestinal barrier function leads to the destruction of intestinal mucosal tissue and causes inflammatory disease[4,5]. However, inflammation might be an important risk factor for the development of colitis-associated CRC[6,7].

It is well known that the intestinal mucosa is exposed to immune and inflammatory stimuli triggered by various pathogenic and oxidative factors[8,9]. Currently, most people believe that intestinal inflammation is caused by a weakened intestinal mucosal barrier and increased permeability of the intestinal mucosa, which leads to the passage of intestinal pathogenic bacteria through the barrier[10-12]. Therefore, intestinal barrier integrity and normal immune function are crucial for maintaining cellular homeostasis[13,14].

Alkaline sphingomyelinase (alk-SMase), which is also called nucleotide pyrophosphatase/phosphodiesterase 7 (NPP7), is specifically expressed in the gut in mammals and in the human liver and is the key enzyme for hydrolyzing phospholipids, such as SM, lysophosphatidylcholine (lyso-PC) and platelet activating factor (PAF), in the intestinal lumen [15,16]. In addition, a recent study reported that alk-SMase might play a role in intestinal immune homeostasis through

the regulation of dendritic cell and T-lymphocyte numbers in mesenteric lymph nodes and both the small and large intestines[17]. Therefore, the potential role of alk-SMase in intestinal inflammation has attracted increasing attention. Sjöqvist *et al*[18] reported that chronic colitis was associated with a reduction in mucosal alk-SMase activity, and the authors first suggested the role of alk-SMase in intestinal inflammation. Several studies have confirmed the anti-inflammatory effects of the enzyme on colitis and colitis-associated carcinogenesis[19-21]. Our previous research showed that alk-SMase deficiency increased autotaxin (NPP2) and upregulated the levels of the proinflammatory factor lysophosphatidic acid in a dextran sulfate sodium (DSS)-induced colitis model. Furthermore, the early increase in PAF could trigger DSS-induced inflammation[20]. However, whether alk-SMase affects specific factors related to the stability and permeability of the intestinal mucosa is still unknown.

In this study, we used alk-SMase gene knockout (KO) mice to further investigate the effect of alk-SMase on intestinal barrier function and mucosal permeability in DSS-induced colitis; DSS is a widely used colitis model because of its simplicity and many similarities with human UC[22]. We identified significant changes in several key molecules related to intestinal stability, permeability and antioxidant activity, thus deepening our understanding of the protective roles of these enzymes in the intestinal tract.

MATERIALS AND METHODS

Animals

Duan's group at Lund University, Sweden generously provided alk-SMase$^{-/-}$ mice generated from mice on a C57BL/6 background[23]. The alk-SMase$^{+/+}$ mice and alk-SMase$^{-/-}$ mice used in the experiments were crossbred from alk-SMase$^{+/-}$ mice. The genotypes of the animals were confirmed by polymerase chain reaction (PCR). All mice were kept in the animal facilities under laboratory conditions (23 °C, 12 h/12 h light/dark, 50% humidity, commercial standard pellets and free access to drinking water). The animal protocol was designed to minimize pain or discomfort. All the experimental animals were anesthetized with isoflurane prior to the operation.

Treatment of mice with DSS

Twelve-week-old mice were provided 3% DSS (MW 36000-50000) (MP Biomedicals, Santa Ana, CA, United States) in their daily drinking water for 4 or 6 d and were fed a normal diet during the induction of acute colitis. The disease activity index (DAI) was measured by examining weight loss, stool consistency and blood in the stool during the experiments according to previous methods[20] (Table 1). After DSS was induced, the mice were anesthetized by isoflurane inhalation, and blood was harvested for subsequent analysis. The organs were removed, and the colon length was measured. Colon tissue sections (0.5 mm) were stained with hematoxylin-eosin, and histopathological examinations were performed by microscopy. Colonic mucosal tissues were scraped for subsequent experiments. For the colitis model treated with tertiary butylhydroquinone (t-BHQ) (Sigma-Aldrich, St Louis, MO, United States), KO mice in the t-BHQ group were intraperitoneally injected with 50 mg/kg/d t-BHQ for 6 d and subsequently sacrificed. The experiments were performed as described above.

Detection of intestinal permeability

A fluorescein isothiocyanate dextran (FITC-D) experiment was performed to examine intestinal permeability. Briefly, on days 0, 4 and 6 after 3% DSS treatment, the mice were administered 4 kDa FITC-D (50 mg/100 g body weight) by gavage and sacrificed after 4 h. Serum was obtained by centrifugation at 1000 × *g* for 15 min, after which the fluorescence of FITC-D was measured with a fluorescence microplate reader at excitation and emission wavelengths of 485 nm and 535 nm, respectively. The concentration of FITC-D in serum was calculated based on the standard curve.

Analysis of lipopolysaccharide in serum and secretory immunoglobulin A in mucosal tissue by enzyme-linked immunosorbent assay

Mouse serum lipopolysaccharide (LPS) concentrations were analyzed using an enzyme-linked immunosorbent assay (ELISA) kit (AndyGene Biotechnology, Beijing, China). An anti-mouse LPS antibody was added to the microporous plate. Serum samples and standards were pipetted into separate wells, followed by the addition of a biotin-conjugated LPS antibody. The LPS in the sample or standard was sandwiched between pairs of antibodies. After the wells were thoroughly washed, HRP-conjugated streptavidin was added. The solution turned blue after the addition of the TMB substrate (HRP catalyzes the enzyme-substrate reaction). The LPS concentration of each serum sample was calculated using the standard curve. Intestinal mucosal tissue was homogenized and centrifuged, after which the proteins were extracted. The supernatant was carefully collected. The level of secretory immunoglobulin A (sIgA) in the intestinal mucosa was assessed by an ELISA kit (AndyGene Biotechnology) according to the manufacturer's instructions.

Assessment of intestinal ultrastructural changes by electron microscopy

Colon sections (0.5 cm) were removed and fixed in 2% glutaraldehyde. After fixation, embedding and staining, 60 nm continuous sections were cut. These sections were stained with 1% uranyl acetate for 20 min and lead citrate for 7 min. The microvilli, cell structure, organelles and cell junctions of intestinal mucosal epithelial cells were observed by electron microscopy.

Table 1 Assessment of the disease activity index scores

Score	Weight loss	Stool consistency	Blood in stool
0	None	Normal pellets	Negative
1	1%-5%	Slight loose but still sharp	Hemoccult positive
2	5%-10%	Loose pellet	Visual slightly bleeding
3	10%-15%	Loose feces and no shape	Obvious bleeding but no adhesion around the anus
4	> 15%	Diarrhea	Gross bleeding and blood incrustation around the anus

Protein isolation and western blotting

Colonic mucosal tissues were first lysed in RIPA buffer and subsequently homogenized on ice using a homogenizer. The supernatants of the homogenates were collected after centrifugation at 13500 × rpm at 4°C for 15 min. Total extracted proteins (50 μg) were separated by sodium-dodecyl sulfate gel electrophoresis, transferred to nitrocellulose membranes and blocked with 5% skim milk for 1 h at room temperature. Afterward, the membranes were incubated with primary antibodies overnight at 4°C. The primary antibodies used were claudin-3 (1:800 dilution) (Abcam, Cambridge, United Kingdom), claudin-5 (1:800 dilution) (Abcam), occludin (1:400 dilution) (Abcam), zonula occludens-1 (ZO-1) (1:500 dilution) (Abcam), nuclear factor erythroid 2-related factor 2 (Nrf2) (1:500 dilution) (Santa Cruz Biotechnology, Dallas, TX, United States) and β-actin (1:8000 dilution). The membranes were washed with TBST buffer three times for 10 min each. Then, the membranes were incubated with the appropriate peroxidase-conjugated secondary antibodies (1:20000 dilution), after which chemiluminescence was detected. ImageJ software was used to measure the optical density of the bands. The expression levels of the target proteins relative to β-actin were calculated.

Total RNA isolation and quantitative real-time reverse transcription-PCR

Total RNA was isolated from colonic mucosal tissues using TRIzol reagent (Invitrogen of Thermo Fisher Scientific, Waltham, MA, United States). To remove the inhibitory effect of DSS on qPCR, the RNA was purified using lithium chloride[24]. RNA concentration and purity were determined by using a Nanodrop (Thermo Fisher Scientific), and RNA integrity was verified by 2% agarose gel electrophoresis. Briefly, the RNA was reverse-transcribed into cDNA using ReverTra Ace qPCR RT Master Mix with gDNA Remover (Toyobo, Osaka, Japan). Real-time PCR was performed according to the instructions of the SYBR Green Real-time PCR Master Mix Kit (Toyobo). The primers used are shown in Table 2. The relative expression levels of the target genes were normalized to that of glyceraldehyde-3-phosphate dehydrogenase (GAPDH)[25,26] in each sample by the $2^{-\Delta\Delta Ct}$ method.

Detection of serum oxidant and antioxidant markers

The concentration of malondialdehyde (MDA) and the activities of superoxide dismutase (SOD) and glutathione peroxidase (GSH-Px) were determined using commercially available kits (Nanjing Jiancheng Bioengineering Institute, Nanjing, China) according to the manufacturer's instructions. The assay for SOD activity was based on its ability to inhibit the oxidation of hydroxylamine by $O_2^{\cdot-}$ produced from the xanthine-xanthine oxidase system. One unit of SOD activity was defined as the amount that reduced the absorbance at 550 nm by 50%. GSH-Px activity was assayed by quantifying the rate of oxidation of reduced glutathione to oxidized glutathione by H_2O_2, as catalyzed by GSH-Px. MDA levels were measured according to the thiobarbituric acid (TBA) method (Nanjing Jiancheng Bioengineering Institute). The method was based on spectrophotometric measurements of the color produced during the reaction of TBA with MDA. MDA concentrations were calculated by measuring the absorbance of TBA reactive substances at 532 nm.

Statistical analysis

The data are presented as the mean ± standard error of the mean. Each experiment was performed in triplicate and independently repeated a minimum of three times, and every experiment was performed with a sample size of no less than 3 mice per group. Statistical significance was assessed using an unpaired Student's *t*-test for 2-group comparisons. Multigroup comparisons were performed using one-way analysis of variance (ANOVA), followed by using the Least Significant Difference test. A P value < 0.05 was considered statistically significant. Data analysis was conducted using SPSS 20.0 software (IBM Corp., Armonk, NY, United States), while graphical representations were created using GraphPad Prism software, version 5 (GraphPad Software, Inc., La Jolla, CA, United States).

RESULTS

alk-SMase (NPP7) deficiency exacerbates DSS-induced colitis

In this study, 3% DSS successfully induced acute colitis in both wild-type (WT) and KO mice. As shown in Figure 1A, the body weights of WT and KO mice were slightly decreased on day 4 but were substantially decreased from day 5 to day 6 of DSS treatment. On day 6, the weight of KO mice decreased by 23.1%, whereas that of WT mice decreased by 14.5%. Similarly, the changes in the DAI scores were consistent with the effects on body weight, and the scores were significantly

Table 2 Quantitative real-time reverse transcription-polymerase chain reaction primers for target genes

Gene	Gene ID	Primer
ZO-1 F	21872	AGCTGCCTCGAACCTCTACTCTAC
ZO-1 R		GCCTGGTGGTGGAACTTGCTC
Occludin F	18260	TGCTTCATCGCTTCCTTAGTAA
Occludin R		GGGTTCACTCCCATTATGTACA
Claudin2 F	12738	GGGCAATCGTACCAACTA
Claudin2 R		CAGTCAGGCTGTATGAGTTG
Claudin3 F	12739	GGCGGCTCTGCTCACCTTA
Claudin3 R		CGTACAACCCAGCTCCCATC
Claudin5 F	12741	TGGTGCTGTGTCTGGTAGGATGG
Claudin5 R		GTCACGATGTTGTGGTCCAGGAAG
Claudin8 F	54420	TGTCTGCCTTCATCGAAAGTAA
Claudin8 R		GGCATGCCTCATACAATTCATC
MUC2 F	17831	TGCTGACGAGTGGTTGGTGAATG
MUC2 R		TGATGAGGTGGCAGACAGGAGAC
Nrf2 F	18024	CGAGATATACGCAGGAGAGGTAAGA
Nrf2 R		GCTCGACAATGTTCTCCAGCTT
HO-1 F	15368	ACCGCCTTCCTGCTCAACATTG
HO-1 R		CTCTGACGAAGTGACGCCATCTG
GSH-Px F	14775	AGGGCTGTGCTGATTGAGAATGTG
GSH-Px R		CTCCTGATGTCCGAACTGGTTGC
GCLc F	14629	ATGTGGACACCCGATGCAGTATT
GCLc R		TGTCTTGCTTGTAGTCAGGATGGTTT
SOD2 F	20656	TCCCAGACCTGCCTTACGACTATG
SOD2 R		CTCCTCGGTGGCGTTGAGATTG
GAPDH F	14433	GGTTGTCTCCTGCGACTTCA
GAPDH R		TGGTCCAGGGTTTCTTACTCC

F: Forward; GAPDH: Glyceraldehyde-3-phosphate dehydrogenase; GCLc: Glutamate-cysteine ligase catalytic subunit; GSH-Px: Glutathione peroxidase; HO-1: Heme oxygenase-1; MUC2: Mucin 2; Nrf2: Nuclear factor erythroid 2-related factor 2; R: Reverse; SOD: Superoxide; ZO-1: Zonula occludens-1.

higher in KO mice than in WT mice on day 6 (Figure 1B). Compared with those of WT mice, the colon lengths of KO mice were significantly shorter before DSS treatment or after DSS treatment for 6 d, as shown in Figure 1C. The changes in tumor necrosis factor-alpha and interleukin-6 levels were significantly higher in KO mice than in WT mice after DSS treatment for 4 d (Figure 1D).

Histopathological changes were characterized, and there were different degrees of epithelial damage, inflammatory cell infiltration, goblet cell depletion and crypt damage (Figure 1E). Before DSS induction, the colonic mucosal epithelium of WT and KO mice was intact, and abundant goblet cells were observed, with a clear mucosal structure and no inflammatory cell infiltration. On day 4 after DSS induction, WT mice exhibited relatively minor epithelial cell damage, reduced goblet cells, mild glandular hyperplasia, and infiltrating inflammatory cells. In contrast, KO mice exhibited extensive infiltration of inflammatory cells in the submucosal layer of connective tissue and a small amount of necrosis and desquamation of mucosal epithelial cells. By day 6, WT mice exhibited disorderly arranged glands, with partial necrosis and loss and a significant decrease in goblet cells. KO mice exhibited disruption of the intestinal epithelial layer, marked vascular dilation, abnormal morphology of goblet cells with a large cellular cavity, and widespread inflammation and inflammatory cells extending to blood vessels, the submucosa, and even the muscle layers.

alk-SMase (NPP7) deficiency increases intestinal mucosal permeability in DSS-induced colitis

To explore why the KO mice had more severe colitis than the WT mice, intestinal permeability after DSS administration was examined by measuring changes in the serum concentration of FITC-D. As shown in Figure 2A, the intestinal

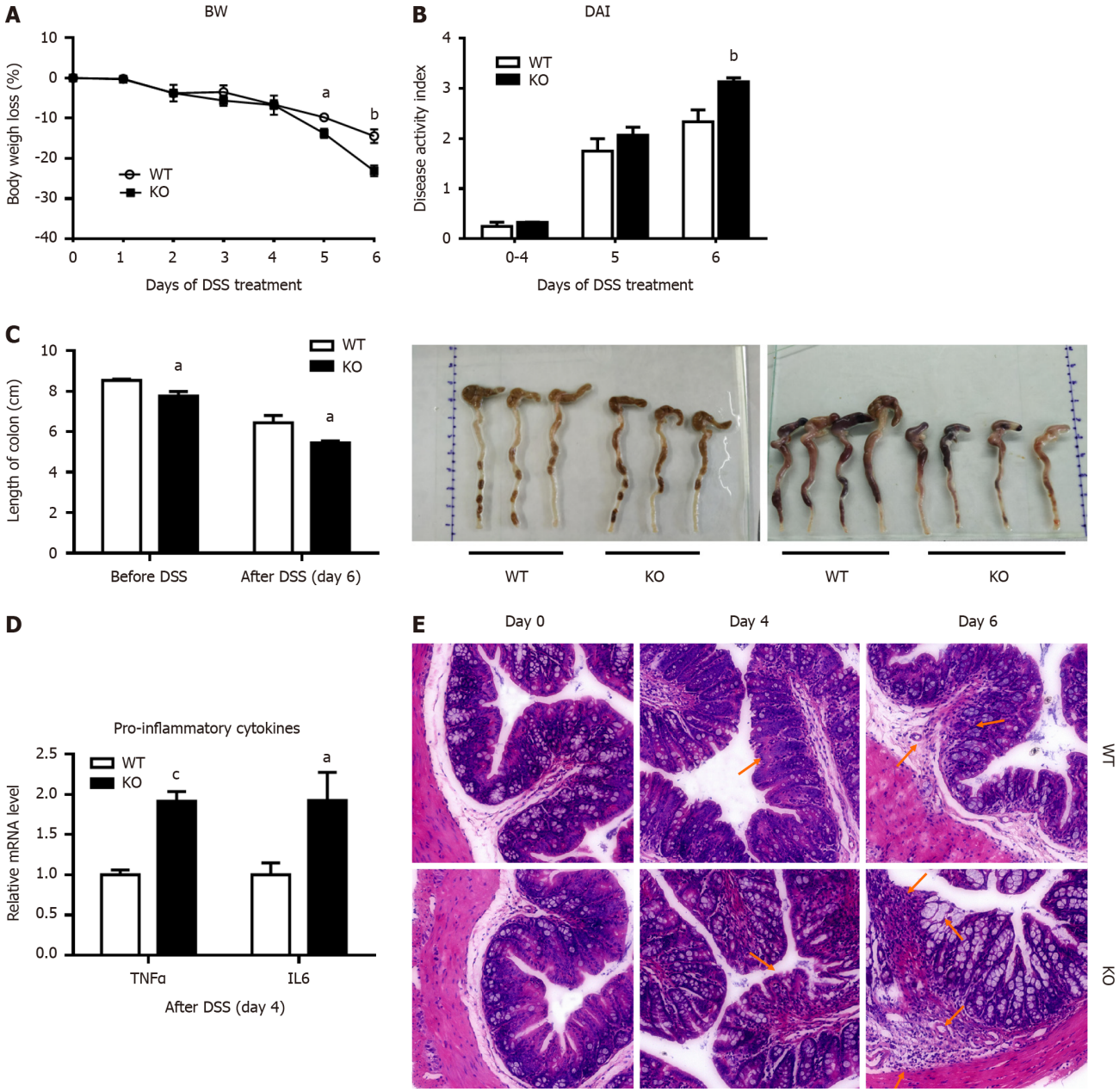

Figure 1 Alkaline sphingomyelinase deficiency exacerbates dextran sulfate sodium-induced colitis in mice. The mice were treated with 3% dextran sulfate sodium (DSS) in drinking water for 6 d. A: Body weight (BW) was measured, and the percentage of BW loss was calculated (n = 6 per group); B: The disease activity index (DAI) was calculated according to the stool bleeding score, BW loss, stool consistency, and disease signs (n = 4 per group); C: After 6 d of DSS treatment, the colon was removed, and the length of the colon was measured (before DSS, n = 3 per group; after DSS, n = 4 per group); D: The mRNA levels of tumor necrosis factor (TNF)-alpha and interleukin (IL)-6 in colonic mucosal tissue were analyzed (n = 4 per group); E: Histopathological characterization of the colon was performed. Arrows: Decreased goblet cells; dysplastic glands; dilated congested blood vessels; destroyed mucosal layer; severe damage to the intestinal epithelium; intensive inflammatory cell infiltration to the submucosa and muscularis. $^{a}P < 0.05$, $^{b}P < 0.01$, $^{c}P < 0.005$ compared with wild-type (WT). KO: Gene knockout.

permeability of WT mice and KO mice did not change before DSS induction. However, on day 4 ($P < 0.005$) and day 6 ($P < 0.05$) after DSS induction, the intestinal permeability of KO mice was significantly higher than that of WT mice. Therefore, we verified that alk-SMase deficiency enhanced intestinal epithelial permeability on day 4 of DSS-induced colitis.

To observe the extent of colonic epithelial cell damage, we compared the levels of the bacterial translocation marker LPS in the serum of WT and KO mice (Figure 2B). We found that the serum concentration of LPS was significantly increased in WT and KO mice after DSS induction, but there was no significant difference between WT and KO mice on day 4, while serum concentrations were significantly higher in KO mice than in WT mice on day 6. The damage to the colonic mucosal epithelial cells in the KO mice had occurred on day 4 and was more severe on day 6.

alk-SMase deficiency changes the expression of intestinal barrier proteins

The expression of ZO-1, occludin, claudin-2, claudin-3, claudin-5 and claudin-8 in mouse colonic mucosal tissues before and after DSS induction was examined. Before DSS treatment (day 0), the mRNA levels of claudin-3 and claudin-8 were

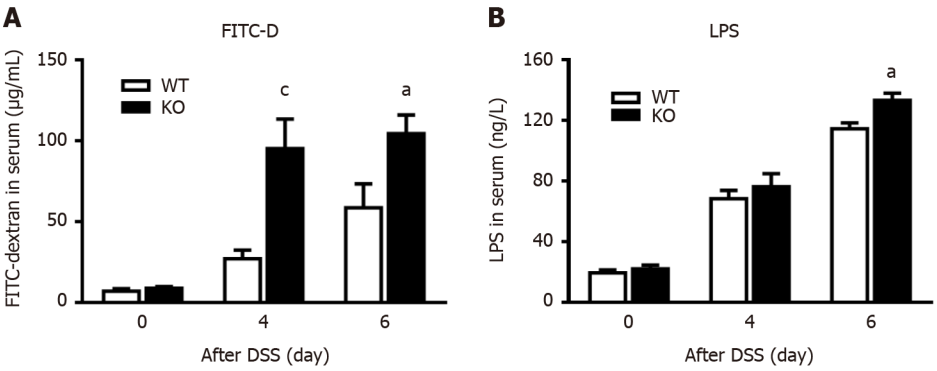

Figure 2 Alkaline sphingomyelinase deficiency increases intestinal permeability in dextran sulfate sodium-induced colitis. The mice were treated with 3% dextran sulfate sodium (DSS) water, and blood was collected on days 0, 4, and 6. A: The mice were administered 4 kDa fluorescein isothiocyanate dextran (FITC-D) by gavage 4 h before blood sampling, after which the fluorescence intensity of FITC-D in serum was measured (n = 5-9 per group); B: Serum lipopolysaccharide (LPS) concentrations were detected on days 0, 4, and 6 after DSS treatment (n = 3 per group). $^{a}P < 0.05$, $^{c}P < 0.005$ compared with wild-type (WT) mice. KO: Gene knockout.

significantly lower in KO mice than in WT mice, but claudin-5 mRNA levels were significantly lower (Figure 3A). However, the mRNA levels in KO mice were significantly lower than those in the WT mice after DSS induction (day 4) (Figure 3B). Western blotting was subsequently performed to detect the protein expression of ZO-1, occludin, claudin-3 and claudin-5. Before DSS treatment (day 0), the expression levels of all the proteins in KO mice were lower than those in WT mice ($P < 0.05$) (Figure 3C). However, after DSS induction for 4 d, the decreases in proteins levels in KO mice were more significant than those in WT mice ($P < 0.01$) (Figure 3D). Furthermore, the level of mucin 2 (MUC2), which is an important secretory protein in the gut, was significantly lower in KO mice than in WT mice on days 0 and 4 after DSS induction. We also examined the levels of the intestinal secretory protein sIgA, which is an important component of the intestinal mucosal immune barrier. On day 4 after DSS induction, sIgA levels were lower in WT and KO mice than before DSS induction, but no significant difference was observed between the two groups. However, on day 6, KO mice exhibited significantly lower levels of sIgA than WT mice, suggesting greater impairment of the intestinal immune barrier in KO mice (Figure 3E and F).

Ultrastructural changes in the colonic epithelial cells of alk-SMase KO mice

As shown in Figure 4, before DSS treatment (day 0), the ultrastructure of colonic mucosal epithelial cells was normal, as shown by electron microscopy. However, there was slight loss of microvilli, swollen mitochondria and impaired tight junctions (TJs) in WT mice and KO mice on day 4 of DSS induction. The damage to the intestinal mechanical barrier in KO mice was more severe than that in WT mice on day 4. Moreover, we found widespread mitochondrial swelling and degeneration in intestinal epithelial cells after DSS induction for 4 d. However, on day 6, compared with WT mice, KO mice exhibited more severe colonic epithelial damage, and the intestinal epithelial cells in KO mice showed abscission of microvilli, widening of intercellular spaces, severe disruption of TJs, nuclear pyknosis, and epithelial ablation, as shown by the arrows in Figure 4.

alk-SMase deficiency decreases antioxidant capacity in vivo

To verify whether mitochondrial damage caused changes in oxidative stress levels, changes in the antioxidant capability of serum were measured after DSS induction for 4 d. There was no difference in the levels of the antioxidant enzymes GSH-Px and SOD before DSS induction, but these levels were significantly lower in KO mice than in WT mice after DSS induction (Figure 5A and B). In contrast, the MOD of KO mice was significantly higher than that of WT mice after DSS induction (Figure 5C).

alk-SMase deficiency attenuates the antioxidant activity of colon tissues

To explore the extent to which antioxidant capacity decreased, changes in the expression of the key transcription factor Nrf2 in colonic mucosal tissues were examined. As shown in Figure 6A and B, the expression of Nrf2 in KO mice was significantly lower than that in WT mice after DSS stimulation for 4 d. Heme oxygenase-1 (HO-1), which is an antioxidant enzyme regulated by Nrf2, was further examined, and the mRNA level in KO mice was significantly lower than that in WT mice. Similarly, on day 4 after DSS treatment, the mRNA levels of GSH-Px, glutamate-cysteine ligase catalytic subunit (GCLc), and SOD in KO mice were significantly lower than those in WT mice (Figure 6C).

Nrf2 activation can rescue the effects of alk-SMase deficiency in colitis

To verify the effect of alk-SMase on the Nrf2 signaling pathway, KO mice were intraperitoneally injected with the Nrf2 activator t-BHQ every day during DSS induction. Body weight loss (Figure 7A), active state, stool consistency and blood in the stool were effectively alleviated by t-BHQ in KO mice. The increased DAI of KO mice after DSS treatment was significantly decreased by t-BHQ-mediated activation of Nrf2 (Figure 7B). Furthermore, the changes in the thymus, spleen, and liver weights caused by the knockout of alk-SMase were significantly reversed to almost the same levels as

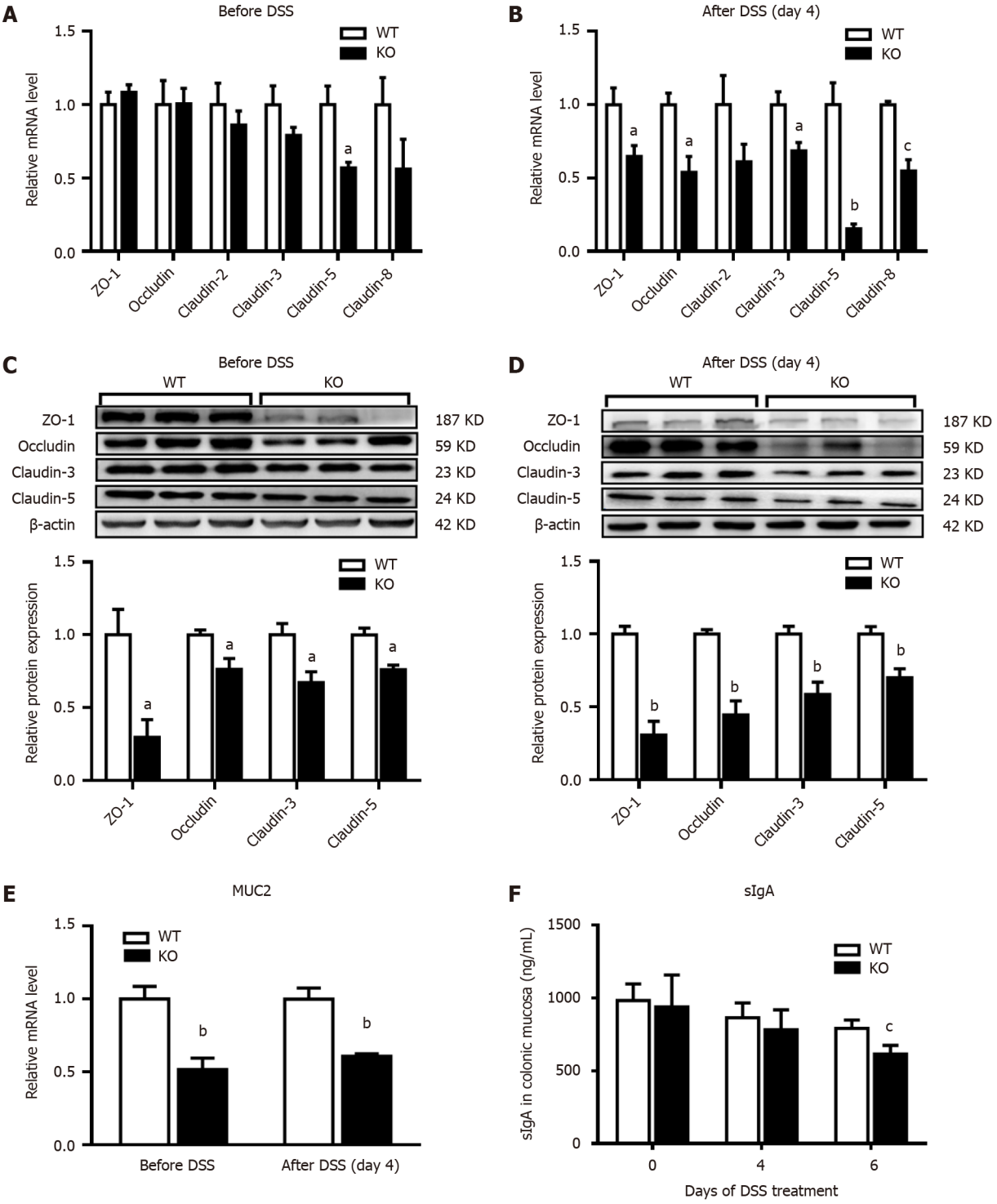

Figure 3 Changes in intestinal mucosal barrier proteins in mice after dextran sulfate sodium induction. The mice were given normal drinking water before dextran sulfate sodium (DSS) treatment, and then the mice were given 3% DSS water for 4 d. Quantitative real-time reverse transcription-polymerase chain reaction and western blot analysis of intestinal barrier proteins were performed on homogenates of colonic mucosa tissues. A and B: The relative mRNA levels were determined relative to those in the wild-type (WT) group; C and D: The densities of the bands were determined relative to those in the WT group; E: Mucin 2 (MUC2) mRNA levels were examined in the homogenates of colonic mucosa tissues; F: The animals were euthanized on days 0, 4, and 6 after receiving DSS water. The levels of secretory immunoglobulin A (sIgA) in the homogenates of colonic mucosa tissues were examined by enzyme-linked immunosorbent assay. n = 3 per group. $^{a}P < 0.05$, $^{b}P < 0.01$, $^{c}P < 0.005$ compared with WT mice. KO: Gene knockout; ZO-1: Zonula occludens-1.

those in WT mice after t-BHQ treatment of experimental colitis (Figure 7C-E). The colons of the KO mice treated with t-BHQ were obviously longer than those of KO mice that were not treated with t-BHQ (Figure 7F).

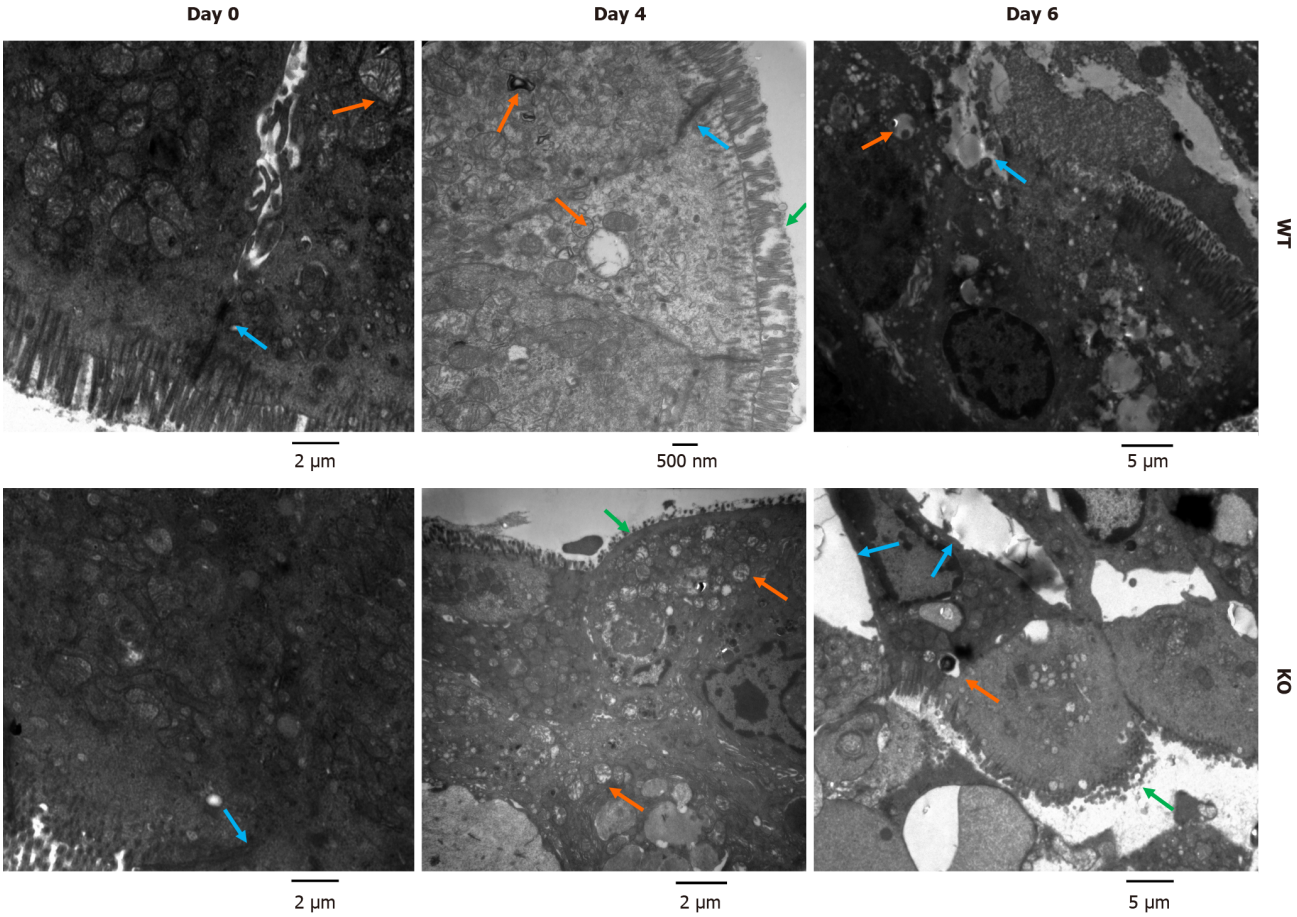

Figure 4 Ultrastructure of colonic mucosal epithelial cells in mice after dextran sulfate sodium induction. Mice were treated with 3% dextran sulfate sodium (DSS) water. Colon sections (0.5 cm) were removed on days 0, 4, and 6 after DSS treatment and fixed in 2% glutaraldehyde. The microvilli, cell structure, organelles and cell junctions of intestinal mucosal epithelial cells were examined by electron microscopy. Before DSS induction, the junctions between epithelial cells in wild-type (WT) and gene knockout (KO) mice were normal. After DSS induction, WT mice exhibited a loss of microvilli, pyknotic nuclei and impaired tight junctions. In KO mice, severe colonic epithelial damage was observed, and the intestinal epithelial cells exhibited damaged microvilli, widening of intercellular spaces, nuclear pyknosis, and mitochondrial swelling and degeneration (green arrows show damaged microvilli, orange arrows show mitochondrial swelling, and blue arrows show the intercellular space).

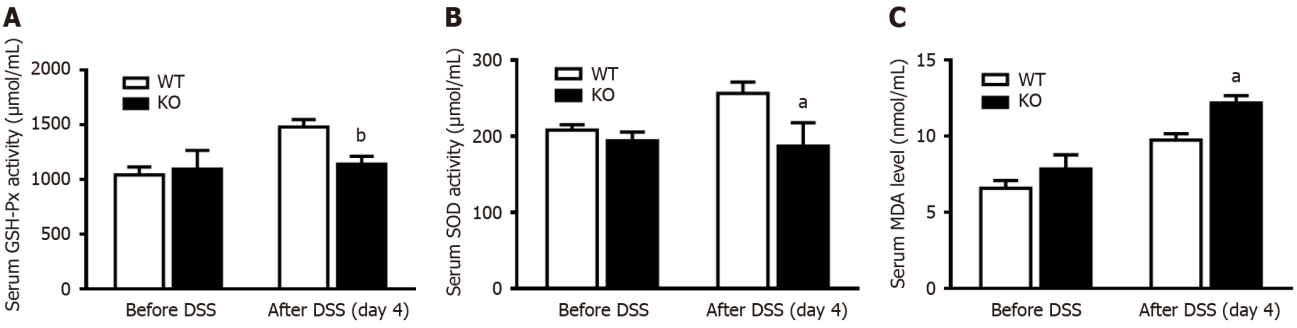

Figure 5 Changes in antioxidant enzyme activity in the serum of mice after dextran sulfate sodium induction. The mice were given normal drinking water before dextran sulfate sodium (DSS) treatment, and the mice were then given 3% DSS water for 4 d. The concentration of malondialdehyde (MDA) and the activities of superoxide (SOD) and glutathione peroxidase (GSH-Px) were determined before and after DSS induction for 4 d. A: Serum MDA levels; B: GSH-Px activity; C: SOD activity. n = 4 per group. $^{a}P < 0.05$, $^{b}P < 0.01$ compared with wild-type (WT) mice. KO: Gene knockout.

DISCUSSION

Alk-SMase is the key enzyme that hydrolyzes SM in the intestinal lumen. It can also hydrolyze many other phospholipids, such as lyso-PC and PAF[15,16]. In this study, alk-SMase KO mice were used to elucidate the pathogenesis of intestinal inflammation in an experimental colitis model and explore the mechanisms underlying the anti-inflammatory effect of alk-SMase. Our results were consistent with those of previous studies, in which weight was lower, the colon was shorter and the DAI was higher in alk-SMase KO mice than in control mice[20]. These findings confirmed that mice with

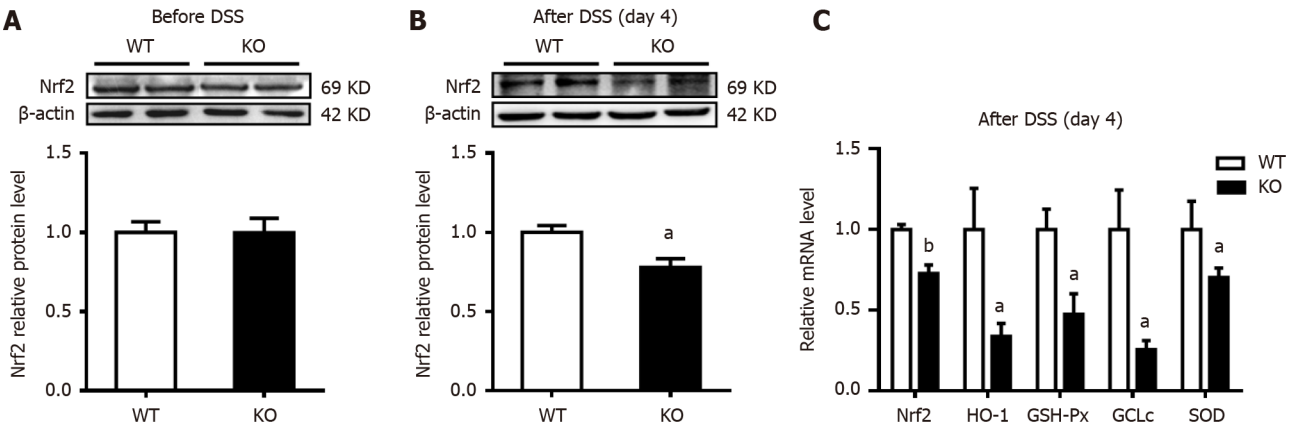

Figure 6 Changes in the expression of colonic nuclear factor erythroid 2-related factor 2 and antioxidant enzymes after dextran sulfate sodium induction. The mice were given normal drinking water before dextran sulfate sodium (DSS) treatment, and the mice were then given 3% DSS water for 4 d. A and B: Western blot analysis of nuclear factor erythroid 2-related factor 2 (Nrf2) was performed on homogenates of colonic mucosa tissues before and after DSS induction; C: Quantitative real-time reverse transcription-polymerase chain reaction was used to measure the mRNA levels of Nrf2 and its target antioxidant genes in colonic mucosa tissues. n = 4 per group. $^{a}P < 0.05$, $^{b}P < 0.01$ compared with wild-type (WT) mice. GCLc: Glutamate-cysteine ligase catalytic subunit; GSH-Px: Glutathione peroxidase; HO-1: Heme oxygenase-1; KO: Gene knockout; SOD: Superoxide.

alk-SMase deficiency developed more severe colitis than normal animals after DSS exposure. In this colitis model, we noticed significant changes in body weight and the DAI score on day 5 after DSS induction and only slight changes in all symptoms on day 4, indicating that intestinal epithelial damage did not occur on day 4. Therefore, it was reasonable to select the fourth day of DSS induction as the time point for follow-up experiments to observe the molecular changes induced by DSS in the intestine[27].

Previous studies have demonstrated the progressive downregulation of alk-SMase activity in patients with chronic UC and colorectal adenocarcinoma[18]. Intestinal alk-SMase has been shown to exert anti-inflammatory effects through the hydrolysis of SM and lyso-PC and inactivation of PAF[16,20,28,29]. However, the specific role of alk-SMase, which is a key enzyme involved in the hydrolysis of phospholipids in intestinal cell membranes, in intestinal barrier function and the underlying mechanism of its anti-inflammatory effect are poorly understood.

To assess damage to the intestinal mucosal barrier, we initially investigated changes in intestinal permeability in mice with DSS-induced colitis by measuring the concentration of FITC-D in the blood, which serves as a reliable indicator of an increase in permeability[30]. We observed a significant increase in FITC-D concentrations in the serum of all the mice following DSS induction, and KO mice exhibited higher levels of FITC-D than WT mice beginning on day 4. These findings suggest that KO mice experience more severe intestinal permeability during the inflammatory response than WT mice, indicating that alk-SMase deficiency exacerbates damage to the intestinal mucosal barrier in a DSS-induced colitis model.

The mechanical barrier of the intestine is crucial for preventing pathogen migration into the mucosa and subsequent inflammation; this barrier consists of TJs, adherens junctions, and desmosomes and plays a crucial role in maintaining the normal permeability of the intestinal mucosa[31]. Proteins such as occludin, claudins, and ZO-1, ZO-2, and ZO-3 are integral components of these junctions[32-34]. Clinical studies have demonstrated that patients with Crohn's disease exhibit decreased protein expression and redistribution of occludin, claudin-3, claudin-5, and claudin-8, while patients with UC exhibit decreased protein expression and redistribution of occludin, claudin-1, and claudin-4[33,34]. The physical and biochemical functions of the intestinal epithelium and its associated mucus layer are important not only for the colonization of beneficial bacteria but also for the maintenance of mucosal immune homeostasis[10].

To evaluate alterations in intestinal permeability, we assessed the expression of various proteins implicated in the integrity of the intestinal mucosal barrier. Our findings revealed that the deletion of alk-SMase in mice resulted in a significant reduction in the protein levels of ZO-1, occludin, claudin-3, and claudin-5 and in the mRNA level of MUC2 before and after DSS induction, indicating that the colonic mucosal barrier was unstable in KO mice that did not receive any inflammatory agents[35,36]. However, when stimulated with an inflammatory agent, the susceptibility of intestinal epithelial cells increased significantly, resulting in exacerbated intestinal barrier function damage in KO mice. Notably, these changes in protein expression were observed on day 4 of DSS treatment and preceded the onset of severe epithelial cell damage induced by DSS. Moreover, the levels of sIgA, an immune protein secreted by intestinal epithelial secretory cells[37], did not significantly change in mucosal tissue on day 4 after DSS induction but did significantly decrease on day 6. This observation suggested that intestinal secretory cells did not experience severe damage on the 4th d but did exhibit damage by the 6th d, which aligns with our initial hypothesis. These findings suggest that alk-SMase plays a critical role in maintaining mucosal barrier function by upregulating the expression of intestinal TJ proteins and mucin secretory molecules during the early stages of inflammation.

Furthermore, we performed electron microscopy to examine the ultrastructure of intestinal epithelial cells. Our observations revealed significant alterations in intercellular junctions, the inflammatory response, and organelles following inflammatory induction, and there were more pronounced changes in alk-SMase KO mice than in WT mice. Notably, alk-SMase-deficient intestinal epithelial cells exhibited substantial damage in the presence of the inflammatory

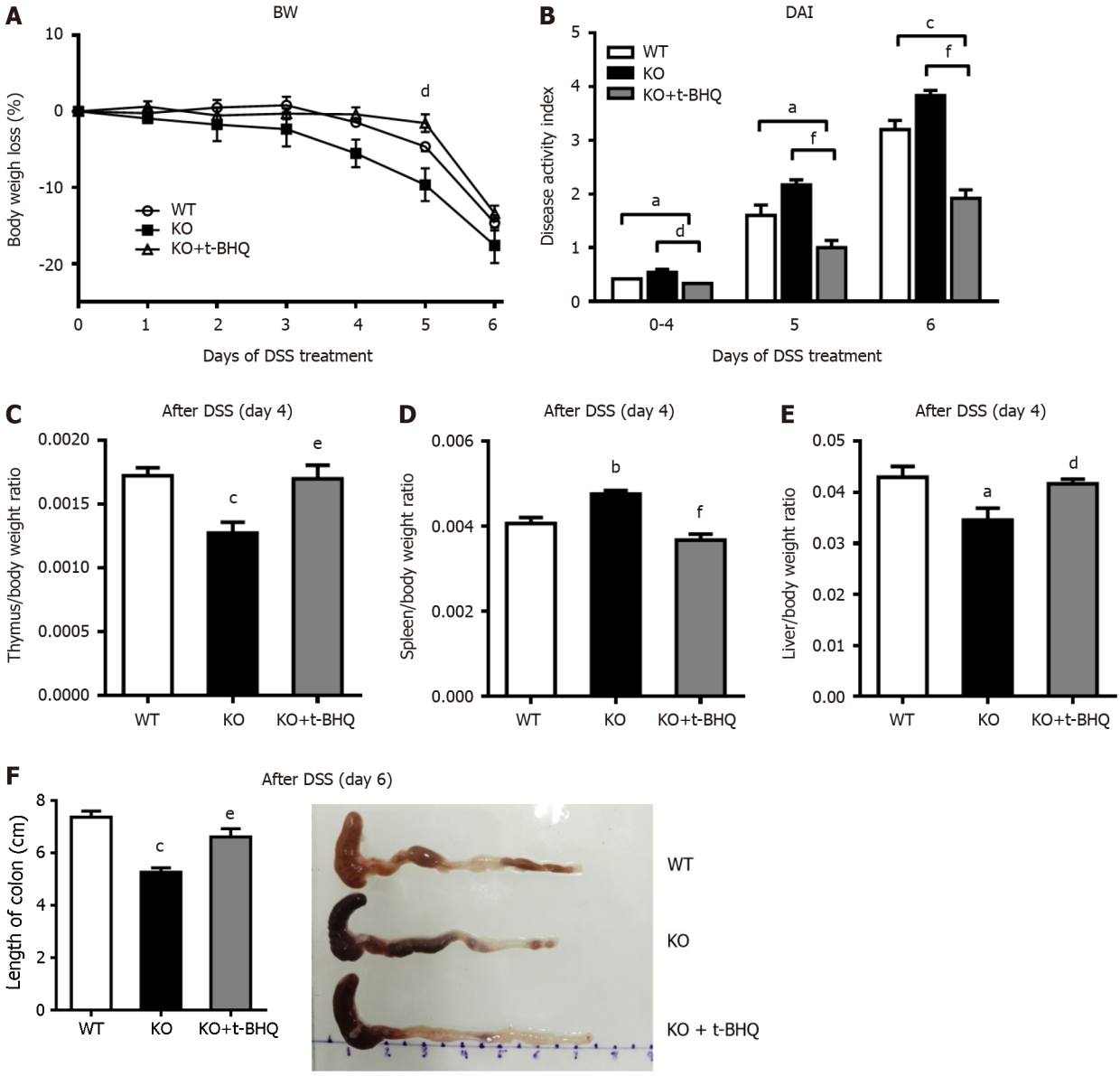

Figure 7 Changes in the incidence of experimental colitis after intraperitoneal injection of tertiary butylhydroquinone in mice. The mice were given 3% dextran sulfate sodium (DSS) drinking water for 6 d, and gene knockout (KO) mice in the tertiary butylhydroquinone (t-BHQ) group were intraperitoneally injected with 50 mg/kg t-BHQ every day. A: Body weight (BW) loss; B: The disease activity index (DAI), calculated according to BW loss, active state, stool consistency, and blood in the stool; C-E: On day 6 of DSS treatment, the mice were killed, the organs were removed and weighed, the ratios of organ weight to BW were calculated; F: The colon lengths were measured. n = 4 or 5 per group. $^{a}P < 0.05$, $^{b}P < 0.01$, $^{c}P < 0.005$, compared to wild-type (WT) mice. $^{d}P < 0.05$, $^{e}P < 0.01$, $^{f}P < 0.005$, compared to KO mice.

agent. These ultrastructural changes provide evidence of intestinal mucosal barrier damage that could lead to increased intestinal permeability. Additionally, during the ultrastructural examination, we observed common mitochondrial swelling in intestinal epithelial cells following DSS-induced inflammation, particularly in the context of alk-SMase deletion, indicating more pronounced mitochondrial degeneration. DSS-induced murine colitis has been previously reported to affect mitochondrial function, resulting in reduced intestinal barrier function and increased permeability[38-40].

To investigate whether alk-SMase exerts protective effects through the mitochondrial antioxidant pathway, we observed changes in the activity of several serum antioxidant enzymes. In general, mitochondria can be stimulated by cellular oxidative stress and produce antioxidants that play a key role in the anti-inflammatory response and in protecting against inflammatory agent invasion[41]. We observed changes in the activities of several serum antioxidant enzymes, such as GSH-Px and SOD, and the serum oxidative stress product MDA; we found that alk-SMase-deficient mice showed greater oxidative stress and decreased antioxidant capacity than WT mice after DSS induction. Several studies have reported the significant roles of SM, PC, and lyso-PC in maintaining intestinal mucosal barrier function and regulating permeability in UC[42-44]. Lipid peroxidation has been suggested to be a mechanism underlying sustained membrane permeability[45]. alk-SMase deficiency disrupts phospholipid metabolism and alters the levels of oxidized lipid molecules, which may contribute to changes in mucosal barrier function and the increase in permeability, thereby

influencing the progression of colon inflammation.

In the DSS-induced colitis model, intestinal inflammation regulates oxidative stress. Our study aimed to investigate the changes in oxidative stress molecules in intestinal mucosal tissue. Nrf2 is a transcription factor that binds to the promoters of downstream genes to upregulate expression and initiate the transcription of oxidative stress-related and anti-inflammatory genes[46,47]. In this study, we observed that alk-SMase regulated Nrf2 expression in colonic mucosal tissues during DSS-induced colitis. This regulation impacted the transcription levels of Nrf2 and its downstream genes, including HO-1, GSH-Px, GCLc, and SOD[48]. The downregulation of these antioxidant enzymes in the colonic mucosal tissues of alk-SMase-deficient mice confirmed the role of alk-SMase in regulating antioxidant capacity by decreasing Nrf2 levels in the DSS-induced colitis model.

The Nrf2 signaling pathway plays a crucial role in gastrointestinal tract function and is directly involved in the development of IBD. Drugs that modulate Nrf2 may be used to treat IBD[49]. Additionally, the previous study demonstrated that t-BHQ reduced intestinal epithelial cell injury and intestinal mucositis *via* activation of Nrf2[50]. To further confirm that alk-SMase regulates intestinal inflammation through the Nrf2 signaling pathway, alk-SMase KO mice with DSS-induced colitis were treated with t-BHQ, an activator of Nrf2[51]. In the present study, DSS inflammatory responses were effectively alleviated, and there were improvements in colonic length, body weight loss, stool bleeding, stool consistency, and disease signs. These results indicated that the downregulation of Nrf2 expression induced by alk-SMase deficiency was reversed.

Additionally, several studies have shown that Nrf2 can strengthen TJs in the intestinal epithelium[52,53]. Activation of the ERK/Nrf2/HO-1 signaling cascade reportedly enhanced the expression of occludin and ZO-1 proteins in the intestinal epithelial layer[54]. Furthermore, Nrf2 has been shown to bind to the promoter regions of certain claudins and increase their expression[55]. In our study, alk-SMase could maintain intestinal permeability, increase antioxidant capacity in colitis mice, and upregulate Nrf2. This effect may be one of the molecular mechanisms underlying the anti-inflammatory effect of alk-SMase. We propose that alk-SMase regulates intestinal mucosal barrier function and antioxidant capacity through the regulation of the Nrf2 signaling pathway. However, further research is needed to explore the relationship between these events and whether alk-SMase exerts anti-inflammatory effects through other pathways.

CONCLUSION

In conclusion, alk-SMase regulates the stability of the intestinal mucosal barrier and enhances antioxidant activity through the Nrf2 signaling pathway.

ARTICLE HIGHLIGHTS

Research background

Ulcerative colitis (UC) is a chronic inflammatory condition of the colon with unknown causes. Alkaline sphingomyelinase (alk-SMase), expressed in intestinal epithelial cells, shows anti-inflammatory effects, but its mechanism remains to be clarified.

Research motivation

This study was motivated by the need to understand the mechanism behind the anti-inflammatory effects of alk-SMase, particularly in relation to intestinal barrier function and oxidative stress in dextran sulfate sodium (DSS)-induced colitis.

Research objectives

The primary objective was to explore how alk-SMase impacts intestinal barrier function and manages oxidative stress, contributing to its anti-inflammatory role in DSS-induced colitis.

Research methods

Mice were given 3% DSS drinking water to induce colitis. The study assessed disease activity, intestinal permeability, bacterial translocation, and the ultrastructure of intestinal epithelial cells. Western blotting and quantitative real-time reverse transcription-polymerase chain reaction were employed to evaluate intestinal barrier proteins and mRNA, and serum oxidant and antioxidant levels were analyzed.

Research results

In gene knockout (KO) mice, inflammation and intestinal permeability were more severe compared to wild-type mice after DSS induction. There was a significant reduction in intestinal barrier proteins and an increase in serum malondialdehyde levels, indicating lower antioxidant capacity. Notably, the administration of the nuclear factor erythroid 2-related factor 2 (Nrf2) activator tertiary butylhydroquinone (t-BHQ) relieved colitis in KO mice.

Research conclusions

This study introduces the model that alk-SMase regulates intestinal barrier stability and antioxidant activity *via* the Nrf2

pathway, offering a new perspective on managing colitis. We employed a novel approach by using alk-SMase KO mice and treating them with t-BHQ to isolate and understand the specific effects of alk-SMase and Nrf2 in colitis.

Research perspectives

The findings underscore the potential of alk-SMase in maintaining intestinal barrier stability and increasing antioxidant capacity, offering insights into novel therapeutic approaches for colitis. Future research will delve into the mechanisms by which alk-SMase influences the Nrf2 pathway, further illuminating its therapeutic potential in colitis.

ACKNOWLEDGEMENTS

The authors would like to acknowledge the laboratory of Harbin Medical University for providing the laboratory space for part of the animal experiments.

FOOTNOTES

Co-first authors: Ye Tian and Xin Li.

Author contributions: Petersen JDD and Zhang P initiated the study; Tian Y, Li X, and Wang X contributed equally to this study; Li X and Wang X conducted the experiments; Tian Y wrote the manuscript; Pei ST, Pan HX, Cheng YQ, and Li YC conducted the preliminary data analysis; Zhang P contributed to the preliminary data analysis supervision; Cao WT reviewed and reanalyzed the data and confirmed the authenticity of the data. All of the authors discussed the results, commented on the manuscript, and approved the publication submission.

Supported by the Natural Science Foundation of Hainan Province, No. 823MS046; and the Talent Program of Hainan Medical University, No. XRC2022007.

Institutional animal care and use committee statement: This study was conducted in strict accordance with ethical guidelines for animal research. All experimental animals were housed in a controlled environment. Isoflurane was used for anesthesia prior to operations to minimize pain and discomfort. The experimental protocols involving animals were carefully designed to reduce suffering and were reviewed and approved by the Ethics Committee of Hainan Medical University (Approval No. HYLL-2022-128).

Conflict-of-interest statement: The authors report no relevant conflicts of interest for this article.

Data sharing statement: No additional data are available. The data for this study are available upon request to the corresponding author pending approval from Hainan Medical University.

ARRIVE guidelines statement: The authors have read the ARRIVE guidelines, and the manuscript was prepared and revised according to the ARRIVE guidelines.

Country/Territory of origin: China

ORCID number: Ping Zhang 0000-0002-0987-4949.

S-Editor: Wang JJ
L-Editor: Filipodia
P-Editor: Yuan YY

REFERENCES

1 **Nagao-Kitamoto H**, Kitamoto S, Kamada N. Inflammatory bowel disease and carcinogenesis. *Cancer Metastasis Rev* 2022; **41**: 301-316 [PMID: 35416564 DOI: 10.1007/s10555-022-10028-4]
2 **Du L**, Ha C. Epidemiology and Pathogenesis of Ulcerative Colitis. *Gastroenterol Clin North Am* 2020; **49**: 643-654 [PMID: 33121686 DOI: 10.1016/j.gtc.2020.07.005]
3 **Guo M**, Wang X. Pathological mechanism and targeted drugs of ulcerative colitis: A review. *Medicine (Baltimore)* 2023; **102**: e35020 [PMID: 37713856 DOI: 10.1097/MD.0000000000035020]
4 **Zhang Y**, Si X, Yang L, Wang H, Sun Y, Liu N. Association between intestinal microbiota and inflammatory bowel disease. *Animal Model Exp Med* 2022; **5**: 311-322 [PMID: 35808814 DOI: 10.1002/ame2.12255]
5 **Chen ML**, Sundrud MS. Cytokine Networks and T-Cell Subsets in Inflammatory Bowel Diseases. *Inflamm Bowel Dis* 2016; **22**: 1157-1167

[PMID: 26863267 DOI: 10.1097/MIB.0000000000000714]
6 **Fantini MC**, Guadagni I. From inflammation to colitis-associated colorectal cancer in inflammatory bowel disease: Pathogenesis and impact of current therapies. *Dig Liver Dis* 2021; **53**: 558-565 [PMID: 33541800 DOI: 10.1016/j.dld.2021.01.012]
7 **Grivennikov SI**. Inflammation and colorectal cancer: colitis-associated neoplasia. *Semin Immunopathol* 2013; **35**: 229-244 [PMID: 23161445 DOI: 10.1007/s00281-012-0352-6]
8 **Dey P**, Chaudhuri SR, Efferth T, Pal S. The intestinal 3M (microbiota, metabolism, metabolome) zeitgeist - from fundamentals to future challenges. *Free Radic Biol Med* 2021; **176**: 265-285 [PMID: 34610364 DOI: 10.1016/j.freeradbiomed.2021.09.026]
9 **Martínez Y**, Más D, Betancur C, Gebeyew K, Adebowale T, Hussain T, Lan W, Ding X. Role of the Phytochemical Compounds like Modulators in Gut Microbiota and Oxidative Stress. *Curr Pharm Des* 2020; **26**: 2642-2656 [PMID: 32410554 DOI: 10.2174/1381612826666200515132218]
10 **Stolfi C**, Maresca C, Monteleone G, Laudisi F. Implication of Intestinal Barrier Dysfunction in Gut Dysbiosis and Diseases. *Biomedicines* 2022; **10** [PMID: 35203499 DOI: 10.3390/biomedicines10020289]
11 **Wang K**, Ding Y, Xu C, Hao M, Li H, Ding L. Cldn-7 deficiency promotes experimental colitis and associated carcinogenesis by regulating intestinal epithelial integrity. *Oncoimmunology* 2021; **10**: 1923910 [PMID: 34026335 DOI: 10.1080/2162402X.2021.1923910]
12 **Barbara G**, Barbaro MR, Fuschi D, Palombo M, Falangone F, Cremon C, Marasco G, Stanghellini V. Inflammatory and Microbiota-Related Regulation of the Intestinal Epithelial Barrier. *Front Nutr* 2021; **8**: 718356 [PMID: 34589512 DOI: 10.3389/fnut.2021.718356]
13 **Okumura R**, Takeda K. Roles of intestinal epithelial cells in the maintenance of gut homeostasis. *Exp Mol Med* 2017; **49**: e338 [PMID: 28546564 DOI: 10.1038/emm.2017.20]
14 **Sharma A**, Rudra D. Emerging Functions of Regulatory T Cells in Tissue Homeostasis. *Front Immunol* 2018; **9**: 883 [PMID: 29887862 DOI: 10.3389/fimmu.2018.00883]
15 **Duan RD**. Alkaline sphingomyelinase: an old enzyme with novel implications. *Biochim Biophys Acta* 2006; **1761**: 281-291 [PMID: 16631405 DOI: 10.1016/j.bbalip.2006.03.007]
16 **Wu J**, Nilsson A, Jönsson BA, Stenstad H, Agace W, Cheng Y, Duan RD. Intestinal alkaline sphingomyelinase hydrolyses and inactivates platelet-activating factor by a phospholipase C activity. *Biochem J* 2006; **394**: 299-308 [PMID: 16255717 DOI: 10.1042/BJ20051121]
17 **Alyamani M**, Kadivar M, Erjefält J, Johansson-Lindbom B, Duan RD, Nilsson Å, Marsal J. Alkaline sphingomyelinase (NPP7) impacts the homeostasis of intestinal T lymphocyte populations. *Front Immunol* 2022; **13**: 1050625 [PMID: 36741374 DOI: 10.3389/fimmu.2022.1050625]
18 **Sjöqvist U**, Hertervig E, Nilsson A, Duan RD, Ost A, Tribukait B, Löfberg R. Chronic colitis is associated with a reduction of mucosal alkaline sphingomyelinase activity. *Inflamm Bowel Dis* 2002; **8**: 258-263 [PMID: 12131609 DOI: 10.1097/00054725-200207000-00004]
19 **Chen Y**, Zhang P, Xu SC, Yang L, Voss U, Ekblad E, Wu Y, Min Y, Hertervig E, Nilsson Å, Duan RD. Enhanced colonic tumorigenesis in alkaline sphingomyelinase (NPP7) knockout mice. *Mol Cancer Ther* 2015; **14**: 259-267 [PMID: 25381265 DOI: 10.1158/1535-7163.MCT-14-0468-T]
20 **Zhang P**, Chen Y, Zhang T, Zhu J, Zhao L, Li J, Wang G, Li Y, Xu S, Nilsson Å, Duan RD. Deficiency of alkaline SMase enhances dextran sulfate sodium-induced colitis in mice with upregulation of autotaxin. *J Lipid Res* 2018; **59**: 1841-1850 [PMID: 30087205 DOI: 10.1194/jlr.M084285]
21 **Andersson D**, Kotarsky K, Wu J, Agace W, Duan RD. Expression of alkaline sphingomyelinase in yeast cells and anti-inflammatory effects of the expressed enzyme in a rat colitis model. *Dig Dis Sci* 2009; **54**: 1440-1448 [PMID: 18989780 DOI: 10.1007/s10620-008-0509-2]
22 **Chassaing B**, Aitken JD, Malleshappa M, Vijay-Kumar M. Dextran sulfate sodium (DSS)-induced colitis in mice. *Curr Protoc Immunol* 2014; **104**: 15.25.1-15.25.14 [PMID: 24510619 DOI: 10.1002/0471142735.im1525s104]
23 **Zhang Y**, Cheng Y, Hansen GH, Niels-Christiansen LL, Koentgen F, Ohlsson L, Nilsson A, Duan RD. Crucial role of alkaline sphingomyelinase in sphingomyelin digestion: a study on enzyme knockout mice. *J Lipid Res* 2011; **52**: 771-781 [PMID: 21177474 DOI: 10.1194/jlr.M012880]
24 **Viennois E**, Chen F, Laroui H, Baker MT, Merlin D. Dextran sodium sulfate inhibits the activities of both polymerase and reverse transcriptase: lithium chloride purification, a rapid and efficient technique to purify RNA. *BMC Res Notes* 2013; **6**: 360 [PMID: 24010775 DOI: 10.1186/1756-0500-6-360]
25 **Yan F**, Wang L, Shi Y, Cao H, Liu L, Washington MK, Chaturvedi R, Israel DA, Wang B, Peek RM Jr, Wilson KT, Polk DB. Berberine promotes recovery of colitis and inhibits inflammatory responses in colonic macrophages and epithelial cells in DSS-treated mice. *Am J Physiol Gastrointest Liver Physiol* 2012; **302**: G504-G514 [PMID: 22173918 DOI: 10.1152/ajpgi.00312.2011]
26 **Bauer C**, Duewell P, Mayer C, Lehr HA, Fitzgerald KA, Dauer M, Tschopp J, Endres S, Latz E, Schnurr M. Colitis induced in mice with dextran sulfate sodium (DSS) is mediated by the NLRP3 inflammasome. *Gut* 2010; **59**: 1192-1199 [PMID: 20442201 DOI: 10.1136/gut.2009.197822]
27 **Cochran KE**, Lamson NG, Whitehead KA. Expanding the utility of the dextran sulfate sodium (DSS) mouse model to induce a clinically relevant loss of intestinal barrier function. *PeerJ* 2020; **8**: e8681 [PMID: 32195049 DOI: 10.7717/peerj.8681]
28 **Li Q**, Chen G, Zhu D, Zhang W, Qi S, Xue X, Wang K, Wu L. Effects of dietary phosphatidylcholine and sphingomyelin on DSS-induced colitis by regulating metabolism and gut microbiota in mice. *J Nutr Biochem* 2022; **105**: 109004 [PMID: 35351615 DOI: 10.1016/j.jnutbio.2022.109004]
29 **Yun CC**. Lysophosphatidic Acid and Autotaxin-associated Effects on the Initiation and Progression of Colorectal Cancer. *Cancers (Basel)* 2019; **11** [PMID: 31323936 DOI: 10.3390/cancers11070958]
30 **González-González M**, Díaz-Zepeda C, Eyzaguirre-Velásquez J, González-Arancibia C, Bravo JA, Julio-Pieper M. Investigating Gut Permeability in Animal Models of Disease. *Front Physiol* 2018; **9**: 1962 [PMID: 30697168 DOI: 10.3389/fphys.2018.01962]
31 **Nighot P**, Ma T. Endocytosis of Intestinal Tight Junction Proteins: In Time and Space. *Inflamm Bowel Dis* 2021; **27**: 283-290 [PMID: 32497180 DOI: 10.1093/ibd/izaa141]
32 **Landy J**, Ronde E, English N, Clark SK, Hart AL, Knight SC, Ciclitira PJ, Al-Hassi HO. Tight junctions in inflammatory bowel diseases and inflammatory bowel disease associated colorectal cancer. *World J Gastroenterol* 2016; **22**: 3117-3126 [PMID: 27003989 DOI: 10.3748/wjg.v22.i11.3117]
33 **Zeissig S**, Bürgel N, Günzel D, Richter J, Mankertz J, Wahnschaffe U, Kroesen AJ, Zeitz M, Fromm M, Schulzke JD. Changes in expression and distribution of claudin 2, 5 and 8 lead to discontinuous tight junctions and barrier dysfunction in active Crohn's disease. *Gut* 2007; **56**: 61-72 [PMID: 16822808 DOI: 10.1136/gut.2006.094375]
34 **Vetrano S**, Rescigno M, Cera MR, Correale C, Rumio C, Doni A, Fantini M, Sturm A, Borroni E, Repici A, Locati M, Malesci A, Dejana E,

Danese S. Unique role of junctional adhesion molecule-a in maintaining mucosal homeostasis in inflammatory bowel disease. *Gastroenterology* 2008; **135**: 173-184 [PMID: 18514073 DOI: 10.1053/j.gastro.2008.04.002]

35 **Liu Y**, Yu X, Zhao J, Zhang H, Zhai Q, Chen W. The role of MUC2 mucin in intestinal homeostasis and the impact of dietary components on MUC2 expression. *Int J Biol Macromol* 2020; **164**: 884-891 [PMID: 32707285 DOI: 10.1016/j.ijbiomac.2020.07.191]

36 **Ma TY**, Nighot P, Al-Sadi R. Tight junctions and the intestinal barrier. In: Physiology of the gastrointestinal tract (sixth edition). United States: Elsevier, 2018: 587-639

37 **Pietrzak B**, Tomela K, Olejnik-Schmidt A, Mackiewicz A, Schmidt M. Secretory IgA in Intestinal Mucosal Secretions as an Adaptive Barrier against Microbial Cells. *Int J Mol Sci* 2020; **21** [PMID: 33291586 DOI: 10.3390/ijms21239254]

38 **Wang A**, Keita ÅV, Phan V, McKay CM, Schoultz I, Lee J, Murphy MP, Fernando M, Ronaghan N, Balce D, Yates R, Dicay M, Beck PL, MacNaughton WK, Söderholm JD, McKay DM. Targeting mitochondria-derived reactive oxygen species to reduce epithelial barrier dysfunction and colitis. *Am J Pathol* 2014; **184**: 2516-2527 [PMID: 25034594 DOI: 10.1016/j.ajpath.2014.05.019]

39 **Amrouche-Mekkioui I**, Djerdjouri B. N-acetylcysteine improves redox status, mitochondrial dysfunction, mucin-depleted crypts and epithelial hyperplasia in dextran sulfate sodium-induced oxidative colitis in mice. *Eur J Pharmacol* 2012; **691**: 209-217 [PMID: 22732651 DOI: 10.1016/j.ejphar.2012.06.014]

40 **Goudie L**, Mancini NL, Shutt TE, Holloway GP, Mu C, Wang A, McKay DM, Shearer J. Impact of experimental colitis on mitochondrial bioenergetics in intestinal epithelial cells. *Sci Rep* 2022; **12**: 7453 [PMID: 35523978 DOI: 10.1038/s41598-022-11123-w]

41 **Chen Y**, Zhou Z, Min W. Mitochondria, Oxidative Stress and Innate Immunity. *Front Physiol* 2018; **9**: 1487 [PMID: 30405440 DOI: 10.3389/fphys.2018.01487]

42 **Schneider H**, Braun A, Füllekrug J, Stremmel W, Ehehalt R. Lipid based therapy for ulcerative colitis-modulation of intestinal mucus membrane phospholipids as a tool to influence inflammation. *Int J Mol Sci* 2010; **11**: 4149-4164 [PMID: 21152327 DOI: 10.3390/ijms11104149]

43 **Sugita M**, Fujie T, Yanagisawa K, Ohue M, Akiyama Y. Lipid Composition Is Critical for Accurate Membrane Permeability Prediction of Cyclic Peptides by Molecular Dynamics Simulations. *J Chem Inf Model* 2022; **62**: 4549-4560 [PMID: 36053061 DOI: 10.1021/acs.jcim.2c00931]

44 **Sukocheva OA**, Lukina E, McGowan E, Bishayee A. Sphingolipids as mediators of inflammation and novel therapeutic target in inflammatory bowel disease. *Adv Protein Chem Struct Biol* 2020; **120**: 123-158 [PMID: 32085881 DOI: 10.1016/bs.apcsb.2019.11.003]

45 **Wiczew D**, Szulc N, Tarek M. Molecular dynamics simulations of the effects of lipid oxidation on the permeability of cell membranes. *Bioelectrochemistry* 2021; **141**: 107869 [PMID: 34119820 DOI: 10.1016/j.bioelechem.2021.107869]

46 **He F**, Ru X, Wen T. NRF2, a Transcription Factor for Stress Response and Beyond. *Int J Mol Sci* 2020; **21** [PMID: 32640524 DOI: 10.3390/ijms21134777]

47 **Piechota-Polanczyk A**, Fichna J. Review article: the role of oxidative stress in pathogenesis and treatment of inflammatory bowel diseases. *Naunyn Schmiedebergs Arch Pharmacol* 2014; **387**: 605-620 [PMID: 24798211 DOI: 10.1007/s00210-014-0985-1]

48 **Audousset C**, McGovern T, Martin JG. Role of Nrf2 in Disease: Novel Molecular Mechanisms and Therapeutic Approaches - Pulmonary Disease/Asthma. *Front Physiol* 2021; **12**: 727806 [PMID: 34658913 DOI: 10.3389/fphys.2021.727806]

49 **Piotrowska M**, Swierczynski M, Fichna J, Piechota-Polanczyk A. The Nrf2 in the pathophysiology of the intestine: Molecular mechanisms and therapeutic implications for inflammatory bowel diseases. *Pharmacol Res* 2021; **163**: 105243 [PMID: 33080322 DOI: 10.1016/j.phrs.2020.105243]

50 **Deng S**, Wu D, Li L, Li J, Xu Y. TBHQ attenuates ferroptosis against 5-fluorouracil-induced intestinal epithelial cell injury and intestinal mucositis *via* activation of Nrf2. *Cell Mol Biol Lett* 2021; **26**: 48 [PMID: 34794379 DOI: 10.1186/s11658-021-00294-5]

51 **Bursley JK**, Rockwell CE. Nrf2-dependent and -independent effects of tBHQ in activated murine B cells. *Food Chem Toxicol* 2020; **145**: 111595 [PMID: 32702509 DOI: 10.1016/j.fct.2020.111595]

52 **Lau WL**, Liu SM, Pahlevan S, Yuan J, Khazaeli M, Ni Z, Chan JY, Vaziri ND. Role of Nrf2 dysfunction in uremia-associated intestinal inflammation and epithelial barrier disruption. *Dig Dis Sci* 2015; **60**: 1215-1222 [PMID: 25399330 DOI: 10.1007/s10620-014-3428-4]

53 **Lechuga S**, Ivanov AI. Disruption of the epithelial barrier during intestinal inflammation: Quest for new molecules and mechanisms. *Biochim Biophys Acta Mol Cell Res* 2017; **1864**: 1183-1194 [PMID: 28322932 DOI: 10.1016/j.bbamcr.2017.03.007]

54 **Liu Y**, Bao Z, Xu X, Chao H, Lin C, Li Z, Liu Y, Wang X, You Y, Liu N, Ji J. Extracellular Signal-Regulated Kinase/Nuclear Factor-Erythroid2-like2/Heme Oxygenase-1 Pathway-Mediated Mitophagy Alleviates Traumatic Brain Injury-Induced Intestinal Mucosa Damage and Epithelial Barrier Dysfunction. *J Neurotrauma* 2017; **34**: 2119-2131 [PMID: 28093052 DOI: 10.1089/neu.2016.4764]

55 **Fan X**, Staitieh BS, Jensen JS, Mould KJ, Greenberg JA, Joshi PC, Koval M, Guidot DM. Activating the Nrf2-mediated antioxidant response element restores barrier function in the alveolar epithelium of HIV-1 transgenic rats. *Am J Physiol Lung Cell Mol Physiol* 2013; **305**: L267-L277 [PMID: 23748533 DOI: 10.1152/ajplung.00288.2012]

Published by **Baishideng Publishing Group Inc**
7041 Koll Center Parkway, Suite 160, Pleasanton, CA 94566, USA
Telephone: +1-925-3991568
E-mail: office@baishideng.com
Help Desk: https://www.f6publishing.com/helpdesk
https://www.wjgnet.com